

ISSN: 0095-8972 (Print) 1029-0389 (Online) Journal homepage: <http://www.tandfonline.com/loi/gcoo20>

Asymmetry in propeller-like trinuclear diphenoxo-bridged $\text{Cu}^{\text{II}}\text{-Ln}^{\text{III}}\text{-Cu}^{\text{II}}$ ($\text{Ln} = \text{La}, \text{Pr}, \text{Nd}$) Schiff base complexes – synthesis, structure and magnetic properties

Beata Cristóvão & Barbara Miroslaw

To cite this article: Beata Cristóvão & Barbara Miroslaw (2015) Asymmetry in propeller-like trinuclear diphenoxo-bridged $\text{Cu}^{\text{II}}\text{-Ln}^{\text{III}}\text{-Cu}^{\text{II}}$ ($\text{Ln} = \text{La}, \text{Pr}, \text{Nd}$) Schiff base complexes – synthesis, structure and magnetic properties, *Journal of Coordination Chemistry*, 68:9, 1602-1615, DOI: 10.1080/00958972.2015.1022166

To link to this article: <http://dx.doi.org/10.1080/00958972.2015.1022166>




View supplementary material 



Accepted author version posted online: 23 Feb 2015.
Published online: 20 Mar 2015.



Submit your article to this journal 



Article views: 109



View related articles 



View Crossmark data 

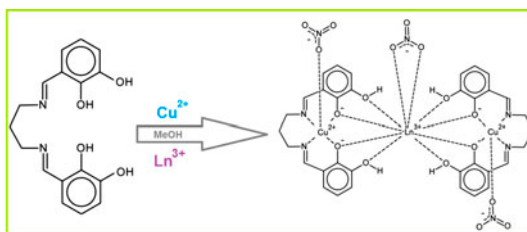
Asymmetry in propeller-like trinuclear diphenoxo-bridged $\text{Cu}^{\text{II}}\text{--Ln}^{\text{III}}\text{--Cu}^{\text{II}}$ ($\text{Ln} = \text{La}, \text{Pr}, \text{Nd}$) Schiff base complexes – synthesis, structure and magnetic properties

BEATA CRISTÓVÃO*[†] and BARBARA MIROSLAW[‡]

[†]Department of General and Coordination Chemistry, Maria Curie-Skłodowska University, Lublin, Poland

[‡]Department of Crystallography, Maria Curie-Skłodowska University, Lublin, Poland

(Received 16 November 2014; accepted 6 February 2015)



Neutral heterotrinuclear complexes $2\{[\text{Cu}_2\text{Ln}(\text{H}_2\text{L})_2(\text{NO}_3)_3]\} \cdot 6\text{CH}_3\text{OH}$ ($\text{Ln} = \text{La}$ (**1**), Nd (**2**)) and $[\text{Cu}_2\text{Ln}(\text{H}_2\text{L})_2(\text{NO}_3)_3] \cdot 4\text{CH}_3\text{OH} \cdot 2\text{H}_2\text{O}$ ($\text{Ln} = \text{Pr}$ (**3**)) were obtained in the reaction of *N,N'*-bis(2,3-dihydroxybenzylidene)-1,3-diaminopropane ($\text{H}_4\text{L} = \text{C}_{17}\text{H}_{18}\text{N}_2\text{O}_4$) with the respective salts of Ln^{III} and Cu^{II} . Compounds **1–3** have similar coordination units and display asymmetry in the degree of planarity of the bridging CuO_2Ln fragments, which is unusual for $\text{Cu}^{\text{II}}\text{--Ln}^{\text{III}}\text{--Cu}^{\text{II}}$ complexes. The geometry of the obtained complexes has been compared to the structural data of other 3d–4f–3d trinuclear diphenoxo-bridged complexes. The temperature dependence of the magnetic susceptibility and the field-dependent magnetization indicate that the interaction between Cu^{II} and Ln^{III} ions is antiferromagnetic for $\text{Ln} = \text{Pr}$ (**2**) and Nd (**3**), whereas in **1** the $\text{Cu}^{\text{II}}\text{--La}^{\text{III}}$ pairs show no significant interaction, which is in accord with the non-magnetic nature of the ground state for lanthanum(III).

Keywords: N,O-donor ligand; Schiff base; Heterotrinuclear complexes; Crystal structure; Magnetic properties

1. Introduction

Investigation of heterometallic compounds containing both 3d and 4f ions is an intensively developing area of research in coordination chemistry. These compounds are of great interest for their structures and useful properties such as magnetic, catalytic, optical, etc. [1–5]. Their coordination architectures depend on many factors, such as coordination geometries

*Corresponding author. Email: beata.cristovao@poczta.umcs.lublin.pl

of the metal ions, nature of the ligands, counter anions and solvent, the ratio of used reagents, etc. [2, 5–8]. Schiff bases as multidentate ligands are very important compounds in these studies. They are easily synthesized and allow good control over the stereochemistry of the metallic centers, as well as over the nuclearity of the complexes, by the suitable choice of the starting substances (aldehyde/ketone and primary amines) [9–17].

N,N'-bis(2,3-dihydroxybenzylidene)-1,3-diaminopropane, H_4L (scheme 1), as a hexadentate Schiff base has an inner smaller site with two N- and two O-donor chelating centers suitable for coordination of metal ions with radii 0.60–0.75 Å e.g. nickel, copper, or zinc ions, and an outer bigger coordination site with four O-donors able to incorporate larger metal ions, radii 0.85–1.06 Å e.g. lanthanide ions. Its unique feature in comparison to other Schiff base ligands is the additional hydroxyl groups that do not undergo deprotonation upon complexation. There is only one report of a crystal structure with this ligand in the heterodinuclear compound of $\text{Cu}^{\text{II}}\text{-Gd}^{\text{III}}$ $\text{LCu}(\text{Me}_2\text{CO})\text{Gd}(\text{NO}_3)_3$ [8]. It crystallizes in the triclinic *P*-1 space group and consists of a 10-coordinate Gd^{III} bridged to a 4-coordinate Cu^{II} ion via two phenolic oxygens of the Schiff base. In this compound, a weak ferromagnetic spin-exchange interaction between Cu^{II} and Gd^{III} was reported. Studies of 3d–4f compounds mainly concentrated on the correlations between molecular structure and magnetic properties. These investigations need to be continued, because of the complex nature of the exchange interaction for systems containing lanthanides [18–22].

We report herein the first heterotrinnuclear $\text{Cu}^{\text{II}}\text{-Ln}^{\text{III}}\text{-Cu}^{\text{II}}$ complexes: $2\{[\text{Cu}_2\text{Ln}(\text{H}_2\text{L})_2(\text{NO}_3)_3]\cdot 6\text{CH}_3\text{OH}$ ($\text{Ln} = \text{La}$ (1), Nd (2)) and $[\text{Cu}_2\text{Ln}(\text{H}_2\text{L})_2(\text{NO}_3)_3]\cdot 4\text{CH}_3\text{OH}\cdot 2\text{H}_2\text{O}$ ($\text{Ln} = \text{Pr}$ (3)) derived from a hydroxy–phenoxy Schiff base ligand (*N,N'*-bis(2,3-dihydroxybenzylidene)-1,3-diaminopropane), and their syntheses, unique structural features, spectroscopic characterization as well as variable-temperature (1.8–300 K) magnetic properties.

2. Experimental

2.1. Materials

All reagents and solvents i.e. $\text{Cu}(\text{CH}_3\text{COO})_2\cdot\text{H}_2\text{O}$, $\text{La}(\text{NO}_3)_3\cdot 6\text{H}_2\text{O}$, $\text{Pr}(\text{NO}_3)_3\cdot 6\text{H}_2\text{O}$, $\text{Nd}(\text{NO}_3)_3\cdot 6\text{H}_2\text{O}$, 1,3-diaminopropane, 2,3-dihydroxybenzaldehyde, and methanol used for synthesis were commercially available and used as received.

2.2. Synthesis

2.2.1. *N,N'*-bis(2,3-dihydroxybenzylidene)-1,3-diaminopropane (H_4L). The Schiff base ($\text{C}_{17}\text{H}_{18}\text{N}_2\text{O}_4$) abbreviated as H_4L was obtained by 2 : 1 condensation of 2,3-dihydroxybenzaldehyde (0.01 M) and 1,3-diaminopropane (0.005 M) in methanol according to the procedure reported earlier [8]. The compound was separated as yellow needles and recrystallized twice from methanol.

2.2.2. $2\{[\text{Cu}_2\text{Ln}(\text{H}_2\text{L})_2(\text{NO}_3)_3]\cdot 6\text{CH}_3\text{OH}$ ($\text{Ln} = \text{La}$ (1), Nd (2)) and $[\text{Cu}_2\text{Ln}(\text{H}_2\text{L})_2(\text{NO}_3)_3]\cdot 4\text{CH}_3\text{OH}\cdot 2\text{H}_2\text{O}$ ($\text{Ln} = \text{Pr}$ (3)). Complexes 1–3 were prepared according to the procedure described below. Methanol solution of copper(II) acetate monohydrate (0.4 mM, 0.0799 g) was added dropwise to a methanol solution (30 mL) of *N,N'*-bis

(2,3-dihydroxybenzylidene)-1,3-diaminopropane, H_4L (0.4 mM, 0.1248 g), to produce a green mixture that was stirred at 45 °C for 30 min. Next, a freshly prepared methanol solution of the respective lanthanide(III) nitrate hexahydrate (5 mL, 0.2 mM, 0.0860 g (salt of La), 0.0870 g (salt of Pr), and 0.0877 g (salt of Nd)) was added slowly to the solution at constant stirring. The resulting deep green mixture was stirred for another 30 min. A small amount of precipitate that appeared was filtered off. Green single crystals suitable for X-ray crystal structure analysis were formed at 4 °C by slow evaporation of the filtrates in the open atmosphere after several weeks.

- (1) Yield: 45%. Elemental analysis for $C_{37}H_{44}N_7O_{20}Cu_2La$ (1172.73). Calcd (%): C, 37.86; H, 3.75; N, 8.36; Cu, 10.83; La, 11.85. Found (%): C, 37.40; H, 3.55; N, 8.20; Cu, 10.40; La, 11.50.
- (2) Yield: 48%. Elemental analysis for $C_{37}H_{44}N_7O_{20}Cu_2Nd$ (1178.13). Calcd (%): C, 37.69; H, 3.73; N, 8.31; Cu, 10.79; Nd, 12.24. Found (%): C, 37.30; H, 3.60; N, 8.10; Cu, 10.50; Nd, 12.00.
- (3) Yield: 40%. Elemental analysis for $C_{38}H_{48}N_7O_{23}Cu_2Pr$ (1242.86). Calcd (%): C, 36.69; H, 4.18; N, 7.89; Cu, 10.23; Pr, 11.34. Found (%): C, 36.30; H, 4.10; N, 7.70; Cu, 10.00; Pr, 10.90.

2.3. Methods

The carbon, hydrogen, and nitrogen contents in the compounds were determined by elemental analyses using a CHN 2400 Perkin-Elmer analyser. The copper and lanthanide contents were established using an ED XRF spectrophotometer (Canberra-Packard). The FTIR spectra of **1–3** were recorded from 4000 to 400 cm^{-1} using an M-80 spectrophotometer (Carl Zeiss Jena). Samples for FTIR spectra were prepared as KBr disks. Magnetic susceptibility measurements were performed on finely ground crystalline samples from 1.8 to 300 K at magnetic field 0.1 T using a Quantum Design SQUID-VSM magnetometer. Field dependences of magnetization were measured at 2 K in an applied field up to 5 T. Corrections are based on subtracting the sample-holder signal and diamagnetic contribution χ_D estimated from the Pascal's constants [23].

2.4. X-ray crystal structure determination

The X-ray diffraction intensities were collected at 293 K for **1** and **2**, and at 100 K for **3** with an Oxford Diffraction Xcalibur CCD diffractometer with graphite-monochromated MoK_α radiation ($\lambda = 0.71073$ Å) using the ω scan technique, with an angular scan width of 1.0°. The programs CrysAlis CCD and CrysAlis Red [24] were used for data collection, cell refinement, and data reduction. The absorption corrections were applied by the multiscan method of Blessing [25]. The structures were solved by direct methods using SHELXS-97 and refined by full-matrix least-squares on F^2 with SHELXL-97 [26] using Olex2 [27]. The C60 of the propyl bridge in isostructural crystals of **1** and **2** was disordered over two positions with site occupancy factor of the major part being 0.60(3) and 0.64(2) for **1** and **2**, respectively. O13 and O14 of one nitrate in **3** were disordered over two positions with site occupancy factor of the major part being 0.52(1). Non-hydrogen atoms except for the disordered atoms, and some of the C and O atoms in solvent molecules in the outer coordination sphere were refined with anisotropic displacement parameters. One non-coordinated

methanol in **1** was refined with the restraint DFIX for C–O distance of 1.34(2) Å. Most of the O-bonded hydrogens were found in the difference Fourier maps and refined isotropically with $U_{\text{iso}} = 1.5 U_{\text{eq}}$ of the O. The hydroxy O-bonded H atoms of the Schiff base were found in the difference Fourier maps, and then refined with DFIX and DANG restraints to fit the proper geometry. Hydrogens of waters in **3** were difficult to locate in the difference Fourier maps and were omitted from the model. All remaining hydrogens were positioned geometrically and allowed to ride on their parent atoms, with $U_{\text{iso}}(\text{H}) = 1.5 U_{\text{eq}}(\text{C}_{\text{methyl}})$ and $1.2 U_{\text{eq}}$ for the rest of the carbons.

3. Results and discussion

3.1. Infrared spectra

The FTIR spectra of **1–3** were compared with the spectrum of the *N,N'*-bis(2,3-dihydroxybenzylidene)-1,3-diaminopropane (H₄L) to obtain information about the binding mode of the ligand to metal ions (table 1). In the recorded spectra of the free ligand, the wide band

Table 1. Selected spectroscopic data of the *N,N'*-bis(2,3-dihydroxybenzylidene)-1,3-diaminopropane (H₄L) and Cu^{II}La^{III}Cu^{II} (**1**), Cu^{II}Nd^{III}Cu^{II} (**2**), and Cu^{II}Pr^{III}Cu^{II} (**3**) complexes.

H ₄ L	1	2	3	Proposed assignments
—	3430 <i>m</i>	3430 <i>m</i>	3412 <i>m</i>	ν(O–H) + ν(C–H)
3200 <i>m, br</i>	—	—	—	ν(O–H) ↔ ν(N–H)
1640 <i>vs</i>	1620 <i>vs</i>	1620 <i>vs</i>	1620 <i>vs</i>	ν(C=N)
1544 <i>m</i>	1568 <i>m</i>	1568 <i>m</i>	1568 <i>m</i>	ν(C=C)
1460 <i>s</i>	1468 <i>s</i>	1468 <i>s</i>	1468 <i>s</i>	ν(C=C) + ν(N–O) _{comp.}
1448 <i>s</i>	—	—	—	ν(C=C) + sc(C–H)
—	1404 <i>w</i>	1404 <i>w</i>	1404 <i>w</i>	sc(C–H)
1396 <i>m</i>	1384 <i>w</i>	1384 <i>w</i>	1384 <i>w</i>	sc(C–H) + ν(CCC)
1356 <i>m</i>	—	—	—	δ(O–H)
—	1308 <i>s</i>	1308 <i>s</i>	1304 <i>s</i>	ν(C–N) + ω(C–H) + ν(N–O)
—	1256 <i>s</i>	1256 <i>s</i>	1256 <i>s</i>	ν(C–O)
1236 <i>vs</i>	1216 <i>s</i>	1216 <i>s</i>	1220 <i>s</i>	ν(C–O) + δ(O–H)
1164 <i>w</i>	1168 <i>w</i>	1168 <i>w</i>	1168 <i>w</i>	ν(C–C) + tw(C–H)
—	1088 <i>w</i>	1088 <i>w</i>	1088 <i>w</i>	δ(C–H) + ν(N–O)
1064 <i>m</i>	1072 <i>w</i>	1072 <i>w</i>	1072 <i>w</i>	Skeletal
—	1048 <i>w</i>	1048 <i>w</i>	1048 <i>w</i>	δ(C–H)
1012 <i>m</i>	—	—	—	δ(C–H)
—	972 <i>w</i>	972 <i>w</i>	972 <i>w</i>	ρ(C–H) + CH ₂ + δ(CCC)
900 <i>w</i>	—	—	—	γ(O–H)
868 <i>w</i>	864 <i>m</i>	864 <i>m</i>	864 <i>m</i>	δ(C–N=C)
—	820 <i>w</i>	820 <i>w</i>	824 <i>w</i>	Ring breath
788 <i>w</i>	784 <i>w</i>	784 <i>w</i>	784 <i>w</i>	γ(C–H) + ν(N–O)
748 <i>vs</i>	744 <i>s</i>	744 <i>s</i>	740 <i>s</i>	γ(C–H)
—	640 <i>w</i>	640 <i>w</i>	640 <i>w</i>	δ(C=C) + ring deform
—	616 <i>w</i>	616 <i>w</i>	616 <i>w</i>	Ring deform
—	556 <i>w</i>	556 <i>w</i>	556 <i>w</i>	ν(M–O)
—	524 <i>w</i>	524 <i>w</i>	524 <i>w</i>	γ(C–H)
504 <i>w</i>	—	—	—	γ(C–H)
476 <i>m</i>	496 <i>w</i>	496 <i>w</i>	500 <i>w</i>	γ(C–H)
—	412 <i>w</i>	412 <i>w</i>	416 <i>w</i>	ν(M–N)

Notes: *vs* – very strong, *s* – strong, *m* – medium, *w* – weak, *br* – broad, *v* – stretching, *δ* – deformation in plane, *sc* – scissoring, *ω* – wagging, *tw* – twisting, *ρ* – rocking, *γ* – deformation out of plane, *as* – asymmetric, and *sym* – symmetric.

with maximum at 3200 cm^{-1} may be ascribed to the O–H and/or N–H stretch, due to the presence of both keto-enol tautomeric forms in the crystal and the formation of strong intramolecular hydrogen bonds $\text{C}=\text{O}\cdots\text{H}\cdots\text{N}=\text{C} \leftrightarrow \text{C}=\text{O}\cdots\text{H}-\text{N}-\text{C}$ [28–33]. Salen-type Schiff bases as N,O-donors are capable of forming coordinate bonds with many metal ions through azomethine, as well as phenolic groups. The strong and sharp band due to the azomethine $\nu(\text{C}=\text{N})$ of free H_4L is observed at 1640 cm^{-1} . In **1–3**, this band is shifted to lower frequency and appears at 1620 cm^{-1} , indicating a decrease in the $\text{C}=\text{N}$ bond order due to coordinate bond formation between Cu^{II} and the imine nitrogen lone pair of the Schiff base [33–37]. It is consistent with the X-ray diffraction results obtained for **1–3**. The metal-nitrogen coordination bond is also confirmed by the new band in the spectra of complexes at *ca.* $412\text{--}416\text{ cm}^{-1}$, assigned to $\nu(\text{Cu}-\text{N})$ [38, 39]. The strong phenolic $\nu(\text{C}-\text{O})$ stretch at 1236 cm^{-1} for free Schiff base ligand is red shifted in **1–3** and appears at $1220\text{--}1216\text{ cm}^{-1}$, confirming the involvement of the phenolic oxygen in the metal–ligand bonding [7, 33, 40]. In the FTIR spectra of **1–3**, the characteristic frequencies of coordinating mono- and bidentate nitrates overlap and appear at 1468, 1304–1308, 1088, and 784 cm^{-1} [7]. In the low-frequency regions, the new band at 572 cm^{-1} can be attributed to $\nu(\text{M}-\text{O})$ [38, 39]. The $\nu(\text{O}-\text{H})$ stretch, arising from the presence of methanol and water and deprotonated hydroxyl groups of the Schiff base, is observed at $3426\text{--}3412\text{ cm}^{-1}$ [7, 38, 41].

3.2. Crystal and molecular structure

The heterotrinnuclear complexes **1** and **2** with general formula $(2\{[\text{Cu}_2\text{Ln}(\text{H}_2\text{L})_2(\text{NO}_3)_3]\}\cdot 6\text{-CH}_3\text{OH})$, where $\text{Ln} = \text{La}$ (**1**), Nd (**2**) are isostructural and crystallize in the triclinic space group $P\bar{1}$ with two neutral coordination units and six methanols in the asymmetric unit. Both units have the same coordination structure, but they are involved in different intermolecular hydrogen bonds. The crystal structure with atom numbering scheme of **1** is shown in figure 1 (the atom labeling scheme is analogous for **2**). The compound of Pr^{III} (**3**) with a formula $[\text{Cu}_2\text{Ln}(\text{H}_2\text{L})_2(\text{NO}_3)_3]\cdot 4\text{CH}_3\text{OH}\cdot 2\text{H}_2\text{O}$ has a very similar neutral coordination unit, but crystallizes in the monoclinic space group $P2_1/c$ with methanol and water in the outer coordination sphere. Its molecular structure with atom numbering scheme is shown in figure 2. The schematic diagrams of **1–3** are given in figure 3. The crystallographic data and experimental details for **1–3** are summarized in table 2. Selected bond distance and angle values for **1**, **2**, and **3** are presented in table 3. The X-ray crystal structure analysis of **1–3** revealed that the coordination modes of the ligand to copper(II) and lanthanide(III) are the same. The difference is in the kind and amount of solvent molecules in the outer coordination sphere (figure S1, see online supplemental material at <http://dx.doi.org/10.1080/00958972.2015.1022166>). The lanthanide(III) and copper(II) ions are bridged via two phenolic oxygens from the hexadentate Schiff base ligand. The external hydroxyl groups closing the outer compartment are protonated and involved in intra- and intermolecular hydrogen bonds (table 4). As shown in figures 1 and 2 in the reported structures, both Cu^{II} cations are five coordinate and have a classical distorted square pyramidal coordination geometry, where the equatorial coordination sites consist of N_2O_2 donors of the hexadentate Schiff base ligands with $\text{Cu}-\text{N}$ and $\text{Cu}-\text{O}$ bond distances $1.965(6)\text{--}2.007(5)\text{ \AA}$ and $1.918(4)\text{--}1.984(4)\text{ \AA}$, respectively (table 3). The axial position is occupied by monodentate nitrate ($d(\text{Cu}-\text{O}) = 2.340(8)\text{--}2.440(5)\text{ \AA}$). In the coordination sphere of the 10-coordinate oxophilic $\text{Ln}(\text{III})$ ion, there are eight oxygens from the two Schiff base ligands and two oxygens from bidentate (η^2 -chelating) nitrate. The $\text{Ln}-\text{O}$ bond lengths vary from *ca.* 2.4 \AA

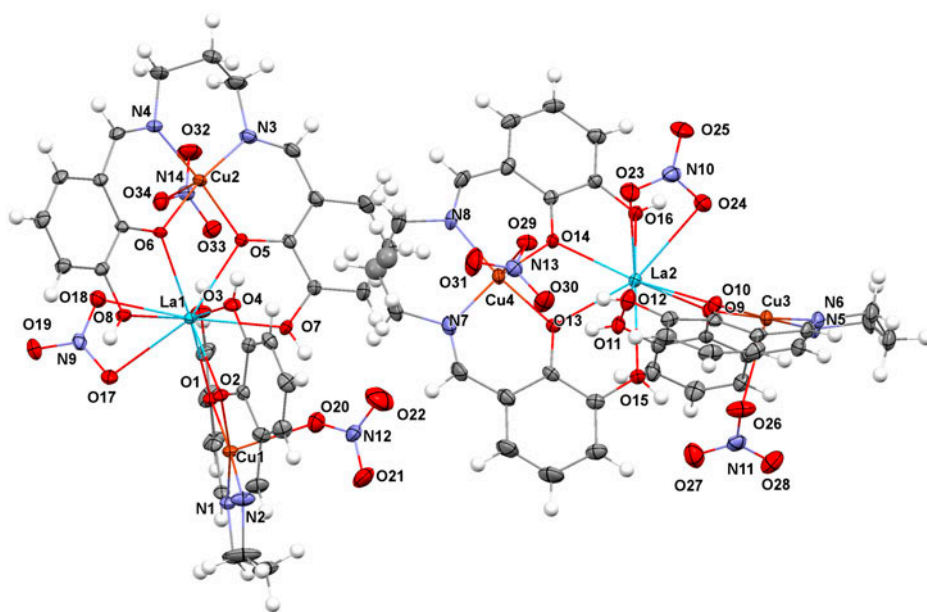


Figure 1. Molecular structure with atom numbering scheme of **1** (analogous for **2**). The outer coordination sphere solvent molecules were omitted for clarity.

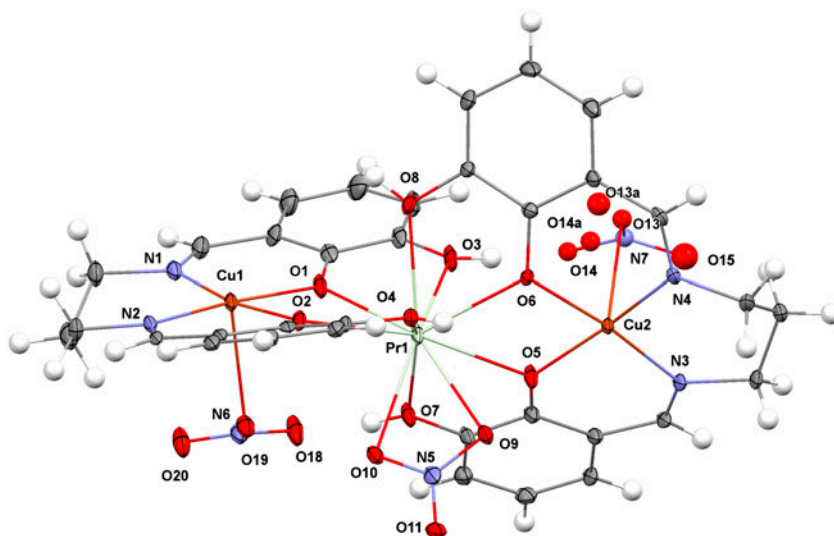


Figure 2. Molecular structure with atom numbering scheme of **3**. The outer coordination sphere solvent molecules were omitted for clarity.

for phenoxo groups located inside the coordination cavity of the Schiff base ligand, through the protonated hydroxy groups closing this cavity, up to *ca.* 2.7 Å for the more loosely connected nitrates (table 3). The intramolecular separations $\text{Cu1}\cdots\text{Ln1}$ and $\text{Cu1}\cdots\text{Cu1}$ are

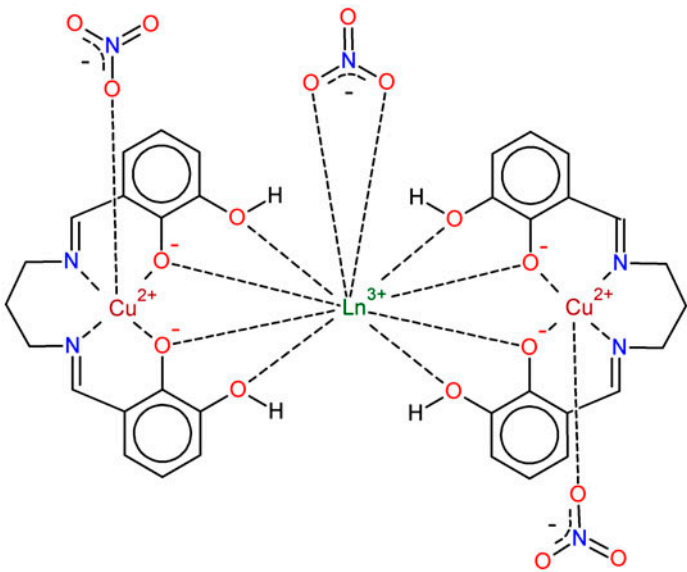


Figure 3. Schematic diagram of heterotrimeric coordination units in 1–3.

Table 2. Crystal data and structure refinement parameters for 1–3.

Identification code	1	2	3
Empirical formula	C ₇₄ H ₈₈ Cu ₄ La ₂ N ₁₄ O ₄₀	C ₇₄ H ₈₈ Cu ₄ N ₁₄ Nd ₂ O ₄₀	C ₃₈ H ₄₈ Cu ₂ N ₇ O ₂₃ Pr
Formula weight	2345.59	2356.25	1242.86
Temperature [K]	293.0	293.0	100.0
Crystal system, space group	Triclinic, <i>P</i> -1	Triclinic, <i>P</i> -1	Monoclinic, <i>P</i> 2 ₁ / <i>c</i>
Unit cell dimensions [Å, °]			
<i>a</i>	11.3083(7)	11.3479(3)	11.7834(4)
<i>b</i>	18.6183(9)	18.4801(5)	23.0244(11)
<i>c</i>	21.6571(9)	21.6915(6)	18.1917(5)
α	80.966(4)	98.453(2)	90
β	87.689(4)	92.788(2)	100.346(3)
γ	89.946(5)	90.412(2)	90
Volume [Å ³]	4499.4(4)	4493.7(2)	4855.3(3)
<i>Z</i> , density _{Calcd} [g cm ⁻³]	2, 1.731	2, 1.741	4, 1.695
Absorption coeff. [mm ⁻¹]	1.956	2.163	1.945
<i>F</i> (0 0 0)	2363.5	2375.8	2520.0
Crystal size [mm]	0.42 × 0.4 × 0.3	0.35 × 0.3 × 0.2	0.3 × 0.3 × 0.1
2 θ range [°]	4.84–50.48	5.36–50.48	5.22–50.48
Refl. collected/unique	31529/16277 [<i>R</i> _{int} = 0.0392]	30101/16235 [<i>R</i> _{int} = 0.0394]	30992/8765 [<i>R</i> _{int} = 0.0525]
Data/restraints/parameters	16277/25/1202	16235/24/1242	8765/12/623
Goodness-of-fit on <i>F</i> ²	1.033	1.049	0.975
Final <i>R</i> indices [<i>I</i> ≥ 2 σ (<i>I</i>)]	<i>R</i> ₁ = 0.0490, <i>wR</i> ₂ = 0.1334	<i>R</i> ₁ = 0.0429, <i>wR</i> ₂ = 0.1060	<i>R</i> ₁ = 0.0494, <i>wR</i> ₂ = 0.1283
Final <i>R</i> indices [all data]	<i>R</i> ₁ = 0.0745, <i>wR</i> ₂ = 0.1531	<i>R</i> ₁ = 0.0648, <i>wR</i> ₂ = 0.1299	<i>R</i> ₁ = 0.0841, <i>wR</i> ₂ = 0.1411
Max/min $\Delta\rho$ [e Å ⁻³]	2.25/–1.26	1.29/–0.84	2.03/–1.43
No. CCSD	1034329	1034330	1034331

Table 3. Selected bond lengths and angles in **1–3** (Å, °).

Bond	1	2	Bond	1	2	Bond	3
Ln1–N9	3.089(5)	3.057(5)	Cu1–N1	2.007(5)	2.004(4)	Cu1–N1	1.977(6)
Ln1–O1	2.560(4)	2.502(3)	Cu1–N2	1.965(6)	1.965(5)	Cu1–N2	1.989(5)
Ln1–O17	2.687(4)	2.654(4)	Cu1–O1	1.929(4)	1.927(3)	Cu1–O1	1.960(4)
Ln1–O18	2.676(4)	2.625(4)	Cu1–O2	1.984(4)	1.990(3)	Cu1–O2	1.947(4)
Ln1–O2	2.500(4)	2.434(3)	Cu1–O20	2.422(5)	2.440(5)	Cu2–O13	2.340(8)
Ln1–O3	2.567(4)	2.516(3)	Cu2–N3	1.971(5)	1.979(4)	Cu2–N3	1.999(5)
Ln1–O4	2.574(4)	2.521(4)	Cu2–N4	1.977(5)	1.981(4)	Cu2–N4	1.970(5)
Ln1–O5	2.511(4)	2.464(3)	Cu2–O5	1.952(4)	1.944(3)	Cu2–O5	1.918(4)
Ln1–O6	2.533(3)	2.476(3)	Cu2–O6	1.942(4)	1.941(3)	Cu2–O6	1.971(3)
Ln1–O7	2.578(4)	2.533(4)	Cu3–N5	1.967(6)	1.975(5)	Pr1–N5	3.104(7)
Ln1–O8	2.601(4)	2.559(3)	Cu3–N6	1.989(5)	1.971(5)	Pr1–O1	2.467(5)
Ln2–N10	3.088(6)	3.067(5)	Cu3–O10	1.923(4)	1.920(4)	Pr1–O10	2.613(5)
Ln2–O10	2.545(4)	2.491(4)	Cu3–O9	1.978(4)	1.962(3)	Pr1–O2	2.454(4)
Ln2–O11	2.590(4)	2.534(4)	Cu4–N7	1.985(6)	1.989(5)	Pr1–O3	2.596(5)
Ln2–O12	2.576(4)	2.534(4)	Cu4–N8	1.979(6)	1.978(5)	Pr1–O4	2.579(4)
Ln2–O13	2.510(4)	2.454(4)	Cu4–O13	1.962(4)	1.962(4)	Pr1–O5	2.514(4)
Ln2–O14	2.514(4)	2.466(3)	Cu4–O14	1.944(4)	1.937(3)	Pr1–O6	2.417(4)
Ln2–O15	2.584(4)	2.537(4)				Pr1–O7	2.518(4)
Ln2–O16	2.586(4)	2.544(4)				Pr1–O8	2.526(4)
Ln2–O23	2.608(5)	2.534(4)				Pr1–O9	2.697(5)
Ln2–O24	2.734(5)	2.748(5)					
Ln2–O9	2.473(4)	2.422(3)					
Dihedral angle	1	2	3				
α Cu1O ₂ Ln1	3.0(2)	2.7(2)	15.2(3)				
α Cu2O ₂ Ln1	17.3(3)	16.7(3)	5.4(2)				
α Cu3O ₂ Ln2	8.4(3)	7.8(2)					
α Cu4O ₂ Ln2	20.4(2)	19.4(2)					

Note: Ln = La (1), Nd (2), Pr (3); α – the dihedral angle between CuO(phenoxo)₂ and LnO(phenoxo)₂ planes.

within the normal range of values for similar polynuclear $\text{Cu}^{\text{II}}\text{-Ln}^{\text{III}}$ compounds, being *ca.* 3.6 and 7.1 Å, respectively [42–45].

The planarity of the bridging CuO₂Ln moiety is estimated by the dihedral angle (α) measured between CuO(phenoxo)₂ and LnO(phenoxo)₂ planes, and has an impact on magnetic properties. In **1–3**, one CuO₂Ln fragment of the trinuclear unit is nearly planar with α values of 3–8°, whereas the second half of the molecule is significantly twisted (α values 15–20°) (table 3). Survey of the Cambridge Structural Database (CSD Version 5.35 with updates May 2014 [46]) revealed 152 diphenoxo-bridged trinuclear 3d–4f–3d structures (table S1, figure 4) in which usually both parts of the coordination unit have the same or very similar structure, with both α angles being nearly equal. The asymmetry occurs only for one $\text{Mn}^{\text{II}}\text{-Gd}^{\text{III}}\text{-Mn}^{\text{II}}$ compound (figure 4) and is observed more frequently for $\text{Zn}^{\text{II}}\text{-Ln}^{\text{III}}\text{-Zn}^{\text{II}}$ trinuclear complexes (table S2, figure 5). These exceptions cover structures where two Schiff base ligand molecules are overlapped one above the other and propeller-like complexes with halides in the coordination sphere of Zn. None of the 30 similar diphenoxo-bridged trinuclear $\text{Cu}^{\text{II}}\text{-Ln}^{\text{III}}\text{-Cu}^{\text{II}}$ complexes found in the CSD display the same degree of asymmetry of the α angle values (table S3, figure 6). The unique feature for the reported hydroxy-substituent ligand-based complexes **1–3** (table 3, figure 6) is probably caused by hydrogen-bonding properties of the external OH groups.

Table 4. Intermolecular interaction parameters in **1–3** (Å, °).

Structure	Donor-H...acceptor	D–H	D...A	H...A	∠DHA
1	O3–H...O33	0.84	2.622(6)	1.80	171
	O4–H...O38 ^a	0.84	2.608(6)	1.78	170
	O7–H...O20	0.84	2.639(7)	1.87	153
	O8–H...O39 ^a	0.83	2.589(6)	1.78	168
	O11–H...O35	0.83	2.597(6)	1.77	176
	O12–H...O30	0.83	2.608(6)	1.79	170
	O15–H...O26	0.84	2.889(8)	2.15	147
	O15–H...O27	0.84	2.962(7)	2.24	145
	O16–H...O40 ^a	0.83	2.549(7)	1.72	171
	O35–H...O27	0.83	2.916(7)	2.11	165
	O36–H...O28	0.82	2.752(7)	2.09	139
	O37–H...O29	0.82	2.922(6)	2.38	124
	O38–H...O37	0.82	2.529(7)	1.83	143
	O39–H...O33	0.82	2.802(6)	2.26	124
	O40–H...O30	0.82	2.731(7)	2.02	145
	O3–H...O33	0.84	2.634(5)	1.80	175
	O4–H...O38 ^a	0.84	2.609(6)	1.78	173
	O7–H...O20	0.83	2.620(6)	1.83	155
	O8–H...O39 ^a	0.83	2.605(6)	1.80	162
	O11–H...O35	0.83	2.603(6)	1.79	168
2	O12–H...O30	0.83	2.641(6)	1.82	172
	O15–H...O26	0.83	2.810(7)	2.09	145
	O15–H...O27	0.83	2.987(8)	2.23	153
	O16–H...O40 ^a	0.83	2.584(7)	1.76	171
	O35–H...O27	0.82	2.881(7)	2.07	170
	O36–H...O28	0.82	2.823(6)	2.05	156
	O37–H...O29	0.82	2.949(7)	2.42	123
	O38–H...O37	0.82	2.668(7)	1.92	152
	O39–H...O33	0.82	2.802(7)	2.26	124
	O40–H...O30	0.82	2.731(7)	2.02	145
	O3–H...O14A	0.84	2.702(7)	1.88	164
	O3–H...O14	0.84	3.516(6)	2.73	156
	O4–H...O16	0.85	2.633(6)	1.78	174
	O7–H...O18	0.85	2.572(7)	1.72	175
	O8–H...O12	0.85	2.579(7)	1.76	164
	O12–H...O21	0.83	2.658(5)	1.87	159
	O16–H...O17	0.82	2.642(6)	1.85	164
	O21–H...O23 ^b	0.83	2.718(6)	2.42	102
	O22–H...O13	0.83	3.497(6)	2.69	165
3	O22–H...O14	0.83	2.870(7)	2.17	143
	O22–H...O13A	0.83	3.351(5)	2.56	160
	O22–H...O14A	0.83	3.516(6)	2.77	151
	O17...O11		2.914(9)		
	O17...O18 ^c		2.702(8)		
	O23...O22		2.251(9)		
	O23...O16 ^d		2.874(9)		

Symmetry codes:

^a $x + 1, + y, + z;$

^b $x, - y + 3/2, z - 1/2;$

^c $1 - x, 1/2 + y, 1/2 - z;$

^d $-x, 1/2 + y, 1/2 - z.$

In the crystal structures of the analyzed complexes, there are many intra- as well as intermolecular hydrogen bonds (figures S2 and S3, table 4). Adjacent molecules are bridged by hydrogen bonds through methanol (**1–3**) and water (**3**). The intermolecular interactions give an extended 3-D network but do not lead to short internuclear contacts.

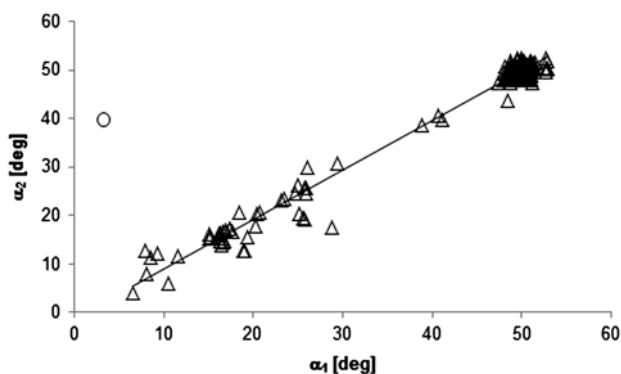


Figure 4. Values of interplanar angles α_1 vs. α_2 (in deg.) in trinuclear complexes of $\text{Tr}^{\text{II}}\text{-Ln}^{\text{III}}\text{-Tr}^{\text{II}}$, where Tr means any transition metal except Zn; α – the dihedral angle between $\text{TrO}(\text{phenoxo})_2$ and $\text{LnO}(\text{phenoxo})_2$ planes; \circ – the values of α_1 and α_2 in $\text{Mn}^{\text{II}}\text{-Gd}^{\text{III}}\text{-Mn}^{\text{II}}$ complex.

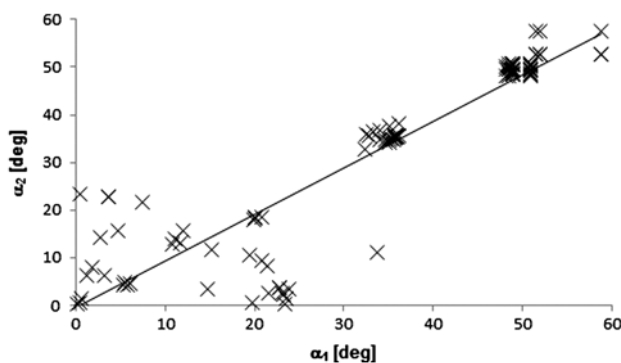


Figure 5. Values of interplanar angles α_1 vs. α_2 (in deg.) in trinuclear complexes of $\text{Zn}^{\text{II}}\text{-Ln}^{\text{III}}\text{-Zn}^{\text{II}}$; α – the dihedral angle between $\text{ZnO}(\text{phenoxo})_2$ and $\text{LnO}(\text{phenoxo})_2$ planes.

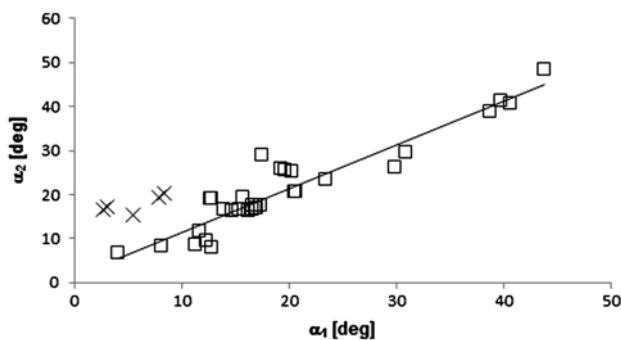


Figure 6. Values of interplanar angles α_1 vs. α_2 (in deg.) in trinuclear complexes of $\text{Cu}^{\text{II}}\text{-Ln}^{\text{III}}\text{-Cu}^{\text{II}}$; α – the dihedral angle between $\text{CuO}(\text{phenoxo})_2$ and $\text{LnO}(\text{phenoxo})_2$ planes; \times – the values of α_1 and α_2 in **1–3**.

3.3. Magnetic properties

Temperature-dependent molar susceptibility measurements of crystalline samples of $\text{Cu}^{\text{II}}\text{--La}^{\text{III}}\text{--Cu}^{\text{II}}$ (**1**), $\text{Cu}^{\text{II}}\text{--Nd}^{\text{III}}\text{--Cu}^{\text{II}}$ (**2**), and $\text{Cu}^{\text{II}}\text{--Pr}^{\text{III}}\text{--Cu}^{\text{II}}$ (**3**) were carried out in an applied magnetic field of 0.1 T from 1.8 to 300 K. The data are presented as plots of $\chi_{\text{M}}T$ versus T , in figure 7, where χ_{M} is the molar magnetic susceptibility and T is the absolute temperature. The magnetic properties of heteronuclear $\text{Cu}^{\text{II}}\text{--Ln}^{\text{III}}$ compounds are governed by three factors: the thermal population of the Stark components of Ln^{III} , the $\text{Cu}^{\text{II}}\cdots\text{Cu}^{\text{II}}$ interactions (including intermolecular interaction), and the $\text{Cu}^{\text{II}}\text{--Ln}^{\text{III}}$ interactions.

At room temperature, the $\chi_{\text{M}}T$ product of $\text{Cu}^{\text{II}}\text{--La}^{\text{III}}\text{--Cu}^{\text{II}}$ (**1**) is $0.740\text{ cm}^3\text{ mol}^{-1}\text{ K}$. This value is close to the theoretically calculated $0.750\text{ cm}^3\text{ mol}^{-1}\text{ K}$ by equation (1) for two uncorrelated Cu^{II} ($3d^9$, $S = 1/2$) ions, since no contribution is expected from the nonmagnetic La^{III} ion ($4f^0$, $S = 0$),

$$\chi_{\text{M}}T = (N\beta^2/3k)2g_{\text{Cu}^2}S_{\text{Cu}}(S_{\text{Cu}} + 1) \quad (1)$$

where N is Avogadro's constant, β is the Bohr magneton, and k is Boltzman's constant. As the temperature decreases, the $\chi_{\text{M}}T$ product remains almost unchanged in magnitude until 1.8 K (figure 7). In this compound, the intramolecular $\text{Cu}\cdots\text{Cu}$ distance is *ca.* 7.2 Å and may preclude any significant magnetic interactions between the copper centers in the heterotrinnuclear unit. The magnetization *versus* field curve of **1** at 2 K is depicted in figure 8. The measurement shows a saturation value of *ca.* $1.9\mu_{\text{B}}$, which is the expected value for two independent $S = 1/2$ systems with $g = 2$.

For $\text{Cu}^{\text{II}}\text{--Nd}^{\text{III}}\text{--Cu}^{\text{II}}$ (**2**), the experimental value of $\chi_{\text{M}}T$ at room temperature of $1.89\text{ cm}^3\text{ mol}^{-1}\text{ K}$ approximately corresponds to the $\chi_{\text{M}}T$ value of $2.39\text{ cm}^3\text{ mol}^{-1}\text{ K}$ theoretically calculated by equation (2) for two Cu^{II} ($3d^9$, $S = 1/2$) and one Nd^{III} ($4f^3$, $J = 9/2$, $S = 3/2$, $L = 6$, $^4\text{I}_{9/2}$) non-interacting metal ions,

$$\chi_{\text{M}}T = ((N\beta^2/3k)[2g_{\text{Cu}^2}S_{\text{Cu}}(S_{\text{Cu}} + 1) + g_{\text{Ln}^2}J_{\text{Ln}}(J_{\text{Ln}} + 1)]) \quad (2)$$

where N is Avogadro's constant, β is the Bohr magneton, and k is Boltzman's constant. In this equation g_{Ln} is the g factor of the ground J terms of Ln^{III} and is expressed as:

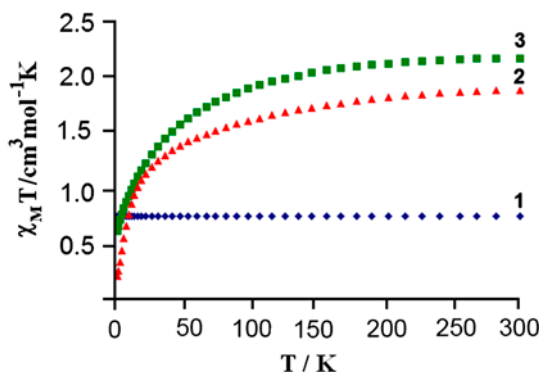


Figure 7. The dependence of experimental $\chi_{\text{M}}T$ vs. T for **1–3**.

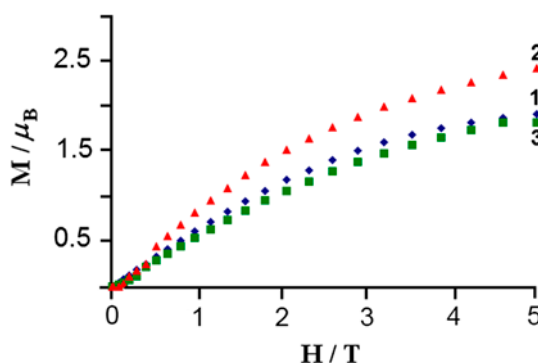
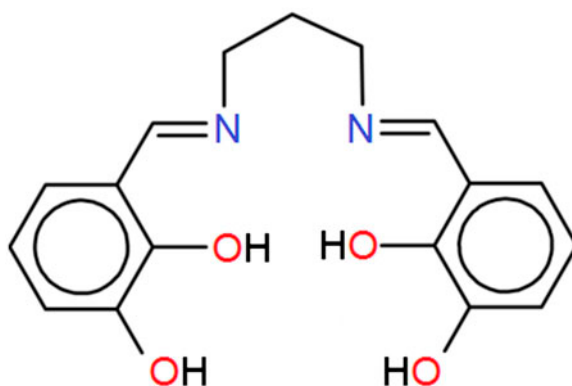


Figure 8. Field dependence of the magnetization for 1–3 at 2 K.



Scheme 1. Schematic diagram of the Schiff base.

$$g_{\text{Ln}} = \frac{3}{2} + \frac{S(S+1) - L(L+1)}{2J(J+1)} \quad (3)$$

For Cu^{II}-Pr^{III}-Cu^{II} (**3**), the experimental value of $\chi_{\text{M}}T$ at room temperature of 2.16 cm³ mol⁻¹ K approximately corresponds to the $\chi_{\text{M}}T$ value of 2.35 cm³ mol⁻¹ K theoretically calculated by equation (2) for two Cu^{II} (3d⁹, $S = \frac{1}{2}$) and one Pr^{III} (4f², $J = 4$, $S = 1$, $L = 5$, ³H₄) isolated paramagnetic metal ions. As depicted in figure 7, the values of $\chi_{\text{M}}T$ decrease by lowering temperature to 0.213 cm³ mol⁻¹ K for **2** and 0.611 cm³ mol⁻¹ K for **3**, respectively, at 1.8 K. This decrease could be caused by crystal field effects, as well as the antiferromagnetic interactions between neighboring Cu^{II} and Ln^{III} ions. The susceptibility data obey the Curie–Weiss law. Negative value of Weiss constants (−19.5 K for **2** and −17.7 K for **3**) could also confirm weak antiferromagnetic exchange coupling between the metal ions. These results are in agreement with the empirical investigations of heterometallic 3d–4f compounds, in which the 4f ions display spin-orbit coupling [45, 47–52]. Unfortunately, the quantitative description of the magnetic properties of heterometallic

complexes containing lanthanide(III) ions is not an easy task, because of the ligand-field effect and spin-orbit coupling of the Ln^{III} ion [47, 48]. To confirm the nature of the ground state of **2** and **3**, we investigated the variation of the magnetization, M , with respect to the field, at 2 K. The results are shown in figure 8, where molar magnetization M is expressed in μ_{B} units. The compounds do not reach saturation in the applied field range and magnetization in 5 T is $2.30 \mu_{\text{B}}$ for **2** and $1.80 \mu_{\text{B}}$ for **3**. This further indicates that the $\text{Cu}^{\text{II}}_2\text{Ln}^{\text{III}}$ systems display an antiferromagnetic coupling. In fact, this study is in good agreement with a theoretical model of Kahn [48] according to the Ln^{III} ions with f^1 – f^6 configurations should exhibit antiferromagnetic coupling.

4. Conclusion

The new heterotrinnuclear coordination compounds of a tetrahydroxy Schiff base ligand (*N,N'*-bis(2,3-dihydroxybenzylidene)-1,3-diaminopropane) have been synthesized in one pot reaction with Ln^{III} and Cu^{II} salts. This is the first report of diphenoxo-bridged trinuclear $\text{Cu}^{\text{II}}\text{--Ln}^{\text{III}}\text{--Cu}^{\text{II}}$ complexes displaying significant asymmetry in the degree of planarity of the bridging CuO_2Ln fragments. This unique feature can be correlated with the formation of hydrogen bonds by the peripherally located protonated OH groups. The results have been compared with data concerning other reported diphenoxo-bridged $\text{M}^{\text{II}}\text{--Ln}^{\text{III}}\text{--M}^{\text{II}}$ coordination systems. Structurally, the new tetrahydroxy Schiff base complexes resemble more the $\text{Zn}^{\text{II}}\text{--Ln}^{\text{III}}\text{--Zn}^{\text{II}}$ systems than the analogous $\text{Cu}^{\text{II}}\text{--Ln}^{\text{III}}\text{--Cu}^{\text{II}}$ complexes. The temperature dependence of the magnetic susceptibility and the field-dependent magnetization indicated that in the crystals the interaction between neighboring Cu^{II} and Ln^{III} ions is antiferromagnetic for $\text{Ln} = \text{Pr}$ and Nd .

Supplementary material

Crystallographic data for **1–3** have been deposited with the Cambridge Crystallographic Data Center: CCDC 1034329–1034331. This data can be obtained free of charge via www.ccdc.cam.ac.uk/data_request/cif, or by emailing data_request@ccdc.cam.ac.uk, or by contacting the Cambridge Crystallographic Data Center, 12 Union Road, Cambridge CB2 1EZ, UK; Fax: +44 1223 336033.

References

- [1] T. Kajiwarra, M. Nakano, K. Takahashi, S. Takaishi, M. Yamashita. *Chem. Eur. J.*, **17**, 196 (2011).
- [2] O. Iasco, G. Novitchi, E. Jeanneau, D. Luneau. *Inorg. Chem.*, **52**, 8723 (2013).
- [3] M. Towatari, K. Nishi, T. Fujinami, N. Matsumoto, Y. Sunatsuki, M. Kojima, N. Mochida, T. Ishida, N. Re, J. Mrozinski. *Inorg. Chem.*, **52**, 6160 (2013).
- [4] G. Cosquer, F. Pointillart, Y. Le Gal, S. Golhen, O. Cador, L. Ouahab. *Chem. Eur. J.*, **17**, 12502 (2011).
- [5] L. Xu, Q. Zhang, G. Hou, P. Chen, G. Li, D.M. Pajerowski, C.L. Dennis. *Polyhedron*, **52**, 91 (2013).
- [6] Y. Ouyang, C.-Z. Xie, J.-Y. Xu, L. Yu, M.-L. Zhang, D.-Z. Liao. *Inorg. Chem. Commun.*, **27**, 166 (2013).
- [7] B. Cristóvão, J. Klak, B. Mirosław. *J. Coord. Chem.*, **67**, 2728 (2014).
- [8] C.T. Zeyrek, A. Elmali, Y. Elerman. *J. Mol. Struct.*, **740**, 47 (2005).
- [9] T. Gao, P.F. Yan, G.M. Li, G.F. Hou, J.S. Gao. *Inorg. Chim. Acta*, **361**, 2051 (2008).
- [10] B. Biswas, P. Raghavaiah, N. Aliaga-Alcalde, J.D. Chen, R. Ghosh. *Polyhedron*, **29**, 2716 (2010).
- [11] T. Gao, P.F. Yan, G.M. Li, J.W. Zhang, W.B. Sun, M. Suda, Y. Einaga. *Solid State Sci.*, **12**, 597 (2010).

- [12] L. Lekha, K. Kanmani Raja, G. Rajagopal, D. Easwaramoorthy. *J. Mol. Struct.*, **1056–1057**, 307 (2014).
- [13] Z.A. Taha, A.M. Ajlouni, W.A. Momani, A.A. Al-Ghzawi. *Spectrochim. Acta, Part A*, **81**, 570 (2011).
- [14] J. Chakraborty, A. Ray, G. Pilet, G. Chastanet, D. Luneau, R.F. Ziessel, L.J. Charbonnière, L. Carrella, E. Rentschler, M.S.E. Fallahe, S. Mitra. *Dalton Trans.*, 10263 (2009).
- [15] N. Brianese, U. Casellato, S. Tamburini, P. Tomasin, P.A. Vigato. *Inorg. Chim. Acta*, **293**, 178 (1999).
- [16] C.H. Li, X.Z. Song, J.H. Jiang, H.W. Gu, L.M. Tao, P. Yang, X. Li, S.H. Xiao, F.H. Yao, W.Q. Liu, J.Q. Xie, M.N. Peng, L. Pan, X.B. Wu, C. Jiang, S. Wang, M.F. Xu, Q.G. Li. *Thermochim. Acta*, **581**, 118 (2014).
- [17] W.B. Sun, P.F. Yan, G.M. Li, J.W. Zhang, H. Xu. *Inorg. Chim. Acta*, **362**, 1761 (2009).
- [18] M.L. Kahn, C. Mathonière, O. Kahn. *Inorg. Chem.*, **38**, 3692 (1999).
- [19] J.P. Costes, F. Dahan, A. Dupuis, J.P. Laurent. *Eur. J. Inorg. Chem.*, **4**, 1616 (1998).
- [20] M. Andruh, I. Ramade, E. Codjovi, O. Guillou, O. Kahn, J.C. Trombe. *J. Am. Chem. Soc.*, **115**, 1822 (1993).
- [21] R. Koner, H.-H. Lin, H.-H. Wie, S. Mohanta. *Inorg. Chem.*, **44**, 3524 (2005).
- [22] A. Jana, S. Majumder, L. Carrella, M. Nayak, T. Weyhermueller, S. Dutta, D. Schollmeyer, E. Rentschler, R. Koner, S. Mohanta. *Inorg. Chem.*, **49**, 9012 (2010).
- [23] G.A. Bain, J.F. Berry. *J. Chem. Educ.*, **85**, 532 (2008).
- [24] Oxford Diffraction. *Xcalibur CCD System, CrysAlis Software System (Version 1.171)*, Oxford Diffraction Ltd., Abingdon (2009).
- [25] R.H. Blessing. *Acta Crystallogr., Sect. A*, **51**, 33 (1995).
- [26] G.M. Sheldrick. *Acta Crystallogr., Sect. A*, **64**, 112 (2008).
- [27] O.V. Dolomanov, L.J. Bourhis, R.J. Gildea, J.A.K. Howard, H. Puschmann. *J. Appl. Crystallogr.*, **42**, 339 (2009).
- [28] Z. Popović, V. Roje, G. Pavlović, D. Matković-Čalogovića, G. Giester. *J. Mol. Struct.*, **597**, 39 (2001).
- [29] A. Elmali, M. Kabak, E. Kavlakoglu, Y. Elerman, T.N. Durlua. *J. Mol. Struct.*, **510**, 207 (1999).
- [30] Z. Popović, G. Pavlović, D. Matković-Čalogovića, V. Roje, I. Leban. *J. Mol. Struct.*, **615**, 23 (2002).
- [31] K. Užarević, M. Rubčić, V. Stilinić, B. Kaitner, M. Cindrić. *J. Mol. Struct.*, **984**, 232 (2010).
- [32] M. Kabak, A. Elmali, Y. Elerman, T.N. Durlua. *J. Mol. Struct.*, **553**, 187 (2000).
- [33] A. Bartyzel. *J. Coord. Chem.*, **66**, 4292 (2013).
- [34] G.-B. Li, X.-J. Hong, Z.-G. Gu, Z.-P. Zheng, Y.-Y. Wu, H.-Y. Jia, J. Liu, Y.-P. Cai. *Inorg. Chim. Acta*, **392**, 177 (2012).
- [35] A.-N.M.A. Alaghaz, B.A. El-Sayed, A.A. El-Henawy, R.A.A. Ammar. *J. Mol. Struct.*, **1035**, 83 (2013).
- [36] R.K. Dubey, P. Baranwal, A.K. Jha. *J. Coord. Chem.*, **65**, 2645 (2012).
- [37] M. Rasouli, M. Morshedi, M. Amirmasr, A.M.Z. Slawin, R. Randall. *J. Coord. Chem.*, **66**, 1974 (2013).
- [38] S.O. Bahaffi, A.A.A. Aziz, M.M. El-Naggar. *J. Mol. Struct.*, **1020**, 188 (2012).
- [39] S. Yadav, M. Ahmad, K.S. Siddiqi. *Spectrochim. Acta, Part A*, **98**, 240 (2012).
- [40] R. Takjoo, A. Hashemzadeh, H.A. Rudbari, F. Nicolò. *J. Coord. Chem.*, **66**, 345 (2013).
- [41] A.A.A. Aziz, A.N.M. Salem, M.A. Sayed, M.M. Aboaly. *J. Mol. Struct.*, **1010**, 130 (2012).
- [42] J.P. Costes, B. Donnadieu, R. Gheorghe, G. Novitchi, J.P. Tuchagues, L. Vendier. *Eur. J. Inorg. Chem.*, **2008**, 5235 (2008).
- [43] J.P. Costes, F. Dahan, A. Dupuis. *Inorg. Chem.*, **39**, 5994 (2000).
- [44] B. Cristóvão, B. Mirosław. *Inorg. Chim. Acta*, **401**, 50 (2013).
- [45] B. Cristóvão, B. Mirosław, J. Klak. *Polyhedron*, **34**, 121 (2012).
- [46] F.H. Allen. *Acta Crystallogr., Sect. B*, **58**, 380 (2002).
- [47] J.P. Costes, F. Dahan, A. Dupuis, J.P. Laurent. *Eur. J. Inorg. Chem.*, **4**, 1616 (1998).
- [48] M. Andruh, I. Ramade, E. Codjovi, O. Guillou, O. Kahn, J.C. Trombe. *J. Am. Chem. Soc.*, **115**, 1822 (1993).
- [49] R. Gheorghe, P. Cucos, M. Andruh, J.P. Costes, B. Donnadieu, S. Shova. *Chem. Eur. J.*, **12**, 187 (2006).
- [50] M.L. Kahn, C. Mathonière, O. Kahn. *Inorg. Chem.*, **38**, 3692 (1999).
- [51] M.L. Kahn, T.M. Rajendiran, Y. Jeannin, C. Mathoniere, O. Kahn. *C. R. Acad. Sci. Paris, Ser. Ilc Chim.*, **3**, 131 (2000).
- [52] C. Benelli, A.J. Blake, P.E.Y. Milne, J.M. Rawson, R.E.P. Winpenny. *Chem. Eur. J.*, **1**, 614 (1995).